Journal of Materials Chemistry C

Revealing Long-Range Orbit-Orbit Interaction between Coherent Light-Emitting Excitons Occurring in Amplified Spontaneous Emission in $CsPbBr_3$ Microstructures

Journal:	*Journal of Materials Chemistry C*
Manuscript ID	TC-ART-02-2021-000728.R1
Article Type:	Paper
Date Submitted by the Author:	01-Apr-2021
Complete List of Authors:	Wang, Miaosheng; University of Tennessee, Materials Science and Engineering Zhang, Jia; University of Tennessee Zhu, Xixiang; University of Tennessee Knoxville College of Engineering Xu, Hengxing; University of Tennessee, Materials Science and Engineering Hu, Bin; The University of Tennessee, Department of Materials Science and Engineering

Revealing Long-Range Orbit-Orbit Interaction between Coherent Light-Emitting Excitons Occurring in Amplified Spontaneous Emission in $CsPbBr_3$ Microstructures

Miaosheng Wang, Jia Zhang, Xixiang Zhu, Hengxing Xu, and Bin Hu*

Joint Institute for Advanced Materials, Department of Materials Science and Engineering, University of Tennessee, Knoxville, Tennessee, 37996, USA

*Corresponding authors:

Bin Hu, E-mail: bhu@utk.edu

Abstract

Amplified spontaneous emission (ASE) has become a common phenomenon in hybrid perovskites by establishing coherent light-emitting excitons. This paper reports a new phenomenon that the long-range orbit-orbit interaction is established through orbital polarizations between coherent light-emitting excitons during the generation of ASE in the $CsPbBr_3$ microrods. Essentially, when the orbital polarizations are optically generated with the same direction between coherent light-emitting excitons by using circularly polarized pumping beam, the ASE amplitude can be largely enhanced by 22.3 %, as compared to the situation when the orbital polarizations are generated with opposite directions by using linearly polarized photoexcitation in the randomly orientated microstructures. This observation provides evidence that the long-range orbit-orbit interaction occurs between coherent light-emitting excitons in ASE. Furthermore, the long-range orbit-orbit interaction between coherent light-emitting excitons is simultaneously increased with the ASE amplitude while increasing pumping fluence. Therefore, the long-range orbit-orbit interaction plays an important role in developing coherent light-emitting excitons towards ASE in metal halide perovskites.

Keywords: Amplified spontaneous emission; Orbital polarizations, Metal halide perovskites; Coherent excitons.

Introduction

Metal halide perovskites have shown attractive amplified spontaneous emission (ASE) and lasing actions with low threshold[1], high optical gain[2], and high quality factor.[3] In general, metal halide perovskites possess tunable bandgap[4, 5], high quantum yield [6, 7], and strong light-matter interaction[8, 9] towards developing ASE. Recently, the continuous-wave operation of ASE and lasing actions in perovskites have been initially realized in low temperature[10, 11] and subsequently in room temperature[12], representing an important development towards developing electrically pumped laser diodes. On the other hand, the light-emitting excitons are generated with strong electron-orbital momentum through the hybridization between the *s* and *p* orbitals from metal and halide elements.[13, 14] Therefore, metal halide perovskites are promising thin-film semiconductors with the possibilities of realizing orbital-tunable light-emitting excitons. In principle, the orbital interaction between light-emitting excitons can be operated through orbital and magnetic polarizations, leading to long-range and short-range orbit-orbit interactions between light-emitting excitons, respectively. Operating long-range and short-range orbit-orbit interactions through orbital and magnetic polarizations provides a unique method to control the optical properties of light-emitting excitons in hybrid perovskites. It has been shown that externally injecting spins can lead to spin-polarized light-emitting excitons in the spontaneous emission regime in hybrid perovskites.[15-17] On the other hand, circularly polarized photoluminescence (PL) was observed in hybrid perovskites ($MAPbBr_3$) at low temperature (10 K) under circularly polarized photoexcitation.[18] This provides direct evidence that the light-emitting excitons can be established with in-phase orbital polarizations during spontaneous emission in hybrid perovskites. We should note that a coherent interaction can be established between light-emitting states to generate an ASE when the pumping beam exceeds the threshold fluence.[19, 20] However, it has become a fundamental issue on whether orbital and magnetic polarizations can play an important role in establishing the coherent interaction between light-emitting excitons carrying both orbital and spin momentums towards developing an ASE in hybrid perovskites.

In this work, we explore the orbit-orbit interaction between coherent light-emitting excitons by using circularly polarized optical pumping during the generation of ASE based on the randomly oriented $CsPbBr_3$ microrods. We have shown in spontaneous emission that the orbit-orbit interaction can occur through orbital and magnetic polarizations between light-emitting excitons,

leading to long-range and short-range orbit-orbit interactions in hybrid perovskites. [21-23] In the spontaneous regime, we have observed that long-range and short-range orbit-orbit interactions can affect the exciton dissociation through dipole-dipole interaction and the spin mixing between bright and dark states through spin-orbital coupling effects. Here, we monitor the ASE amplitude while optically operating the long-range and short-range orbit-orbit interactions by using circularly and linearly polarized photoexcitations (σ^+ and σ^0). It is observed that a circularly polarized optical excitation can generate a higher ASE amplitude as compared to a linearly polarized optical excitation at the same pumping fluence in the $CsPbBr_3$ microrods, leading to a positive ΔASE phenomenon at room temperature. Increasing the pumping fluence causes an increase in the ΔASE magnitude, proportionally following the ASE trend. This observation provides direct evidence that long-range orbit-orbit interaction is established through orbital polarizations between coherent light-emitting excitons towards developing ASE in the $CsPbBr_3$ microrods. Essentially, this indicates that operating the long-range orbit-orbit interaction plays an important role in establishing coherent light-emitting excitons towards developing an ASE in hybrid perovskites.

Results

Inorganic cesium lead perovskite ($CsPbX_3$) nanostructures have emerged as a very promising gain medium system for developing lasing actions.[1, 24, 25] Meanwhile, the $CsPbX_3$ perovskites exhibit superior thermal and moisture stability to avoid photodegradation in lasing applications.[26] In this work, the randomly oriented $CsPbBr_3$ microrods structure was selected as the gain medium to explore spin-polarized coherent light-emitting excitons in the ASE regime. As shown by the optical microscopy images in Figure 1a, the $CsPbBr_3$ microrods exhibit a rectangular shape with the size of a few μm. The magnified image of a single microrod is shown in Figure S1. Figure 1b shows the PL spectrum peaked at 533 nm with narrow full width at half maximum (FWHM) of 23 nm.

Figure 2a shows the emission spectra from the $CsPbBr_3$ microrods excited by the 343 nm pulse laser with a duration of 290 fs at different pumping intensities. The broad spontaneous emission peaked at 533 nm can be observed at the low pumping intensities. As the pumping fluence was increased, a spectral narrowing phenomenon was observed with a sharp peak at 543 nm above the long-wavelength side of the broad spontaneous emission. Therefore, the sharp emission peak is

not induced by the emission from the potential nanostructure of the $CsPbBr_3$ in the sample with the quantum confinement. Although we cannot completely exclude the possibility of size distribution induced broadening of lasing emission, this pumping intensity-induced spectral narrowing phenomenon clearly represents an ASE in the randomly orientated $CsPbX_3$ microrods. The red-shifted ASE peak with respect to the PL peak has been observed in the $CsPbX_3$ nanocrystals, which is believed to originate from the self-absorption during the single exciton process.[27, 28] Figure 2b illustrates the spectral intensity and width as a function of pumping fluence. The emission intensity was largely increased while the FWHM was decreased to around 10 nm when the pumping fluence was gradually increased above the threshold of 10.2 μJ/cm^2. Figure 2c shows the emission dynamics for the ASE region peaked at 543 nm and the PL region at 530 nm with a pumping fluence of 9 μJ/cm^2, right below the ASE threshold. It can be seen that, below the pumping threshold (12 μJ/cm^2), the PL targeted at spontaneous and ASE regions exhibit similar lifetimes of 2.21 ns and 2.02 ns at 530 nm and 543 nm, respectively. When the pumping fluence is above this threshold, the average lifetime monitored at 543 nm within the ASE region is significantly reduced to 0.36 ns with the fast decay component of 51 ps directly related to ASE and the slow decay component of 1.65 ns. At the same time, the PL peaked at 530 nm within the broad spontaneous region shows an average lifetime of 1.63 ns (Figure 2d). The rapid decay of ASE indicates a stimulated light-emitting process occurring in the ASE region above the pumping threshold.

To identify the orbit-orbit interaction occurring between coherent light-emitting excitons within the ASE regime, we monitored the ASE intensity while optically operating orbit-orbit interaction with in-phase and out-phase orbital and magnetic polarizations between coherent light-emitting excitons by circularly and linearly polarized pumping beams with the same intensity. Here, an exciton can be considered as the pair between an electron from **J** = 1/2 at conduction band minimum and a hole from **S** = 1/2 at valence band maximum. Essentially, an exciton possesses (i) transition dipole (h→e), (ii) orbital momentum (**L**), and (iii) spin momentum (**S**). When an optical excitation meets the bandgap, the polarization of the incident electromagnetic wave can operate the electron-orbital momentum. It should be noted that a circularly polarized pumping beam (σ^+) generates the light-emitting excitons with same-directional electron-orbital and magnetic polarizations, leading to in-phase orbital polarizations between excitons. In contrast, a linearly polarized pumping beam ($\sigma^0 = \sigma^+ + \sigma^-$) gives rise to opposite-directional electron-orbital and

magnetic polarizations, generating out-phase orbital polarizations between light-emitting excitons.[21, 22] With the in-phase relationship under circularly polarized photoexcitation (Figure 3 a), the same-directional orbital polarizations can increase the coherent interaction between excitons. However, the same-directional magnetic polarizations can contribute to spin-orbital coupling between excitons, consequently increasing spin mixing to convert bright excitons to dark excitons through spin scattering. With the out-phase relationship under linearly polarized photoexcitation (Figure 3 b), the opposite-directional orbital polarizations can cause a de-phasing behavior through dipole-dipole interaction, decreasing the coherent interaction between excitons. The opposite-directional magnetic polarizations can then decrease the spin-orbital coupling between excitons, decreasing the spin mixing to convert bright excitons into dark excitons. Clearly, monitoring the ASE with circularly and linearly polarized pumping beams provides an experimental method to identify the orbit-orbit interactions between coherent light-emitting excitons. Here, the ΔASE generated by switching the pumping from linear to circular polarization is defined by $\Delta ASE=(I_{ASE/Circular}- I_{ASE/Linear})/(I_{ASE/Linear}-I_{PL@543nm})$, where $I_{ASE/Circular}$ and $I_{ASE/Linear}$ are the ASE intensity at 543 nm under circularly and linearly polarized photoexcitation, respectively. The subtracted spontaneous emission background under ASE conditions, labeled as $I_{PL@543nm}$, is calculated by using the measured $\boldsymbol{a}\times I_{PL@530nm}$, where the ratio $\boldsymbol{a}$ is derived from the $I_{PL@543nm}/ I_{PL@530nm}$ under the low excitation condition below the ASE threshold. Therefore, we can identify the orbit-orbit interactions between coherent light-emitting excitons by using the ΔASE phenomenon upon switching the pumping beam between linear and circular polarizations.

Figure 4 shows the ASE (peaked at 543 nm) and spontaneous emission (peaked at 530 nm) while the 343 nm pumping beam is switched between linear and circular polarization with identical intensity for each pumping fluence in the $CsPbBr_3$ microrods. We can see in Figure 4a that, under the pumping fluence of 9 μJ/cm^2 below the ASE threshold, the PL intensity shows a limited change upon switching the pumping between linear and circular polarizations in the spontaneous region, giving rise to a negligible ΔPL. When the pumping fluence is increased to 12 μJ/cm^2 above the ASE threshold, circularly and linearly polarized pumping generate higher and lower ASE signals, respectively, leading to positive + ΔASE with the amplitude of 22.3 %. At the same time, the PL intensity still shows a limited change upon switching the pumping between linear and circular polarizations. Due to the random distribution of the $CsPbBr_3$ microrods, the ΔASE is independent

of the sample orientation. This ΔASE phenomenon provides two critical experimental indications. First, the relaxation lifetime of orbit-orbit interaction between coherent light-emitting excitons is comparable with the ASE lifetime in the ps regime. This satisfies the precondition that orbit-orbit interaction between coherent light-emitting excitons can change the ASE, identified by ΔASE phenomenon. Second, the positive sign of ΔASE caused by switching the pumping beam from linear to circular polarization provides evidence that the long-range orbit-orbit interaction is indeed established through orbital polarizations between coherent light-emitting excitons during the generation of ASE. Furthermore, when the pumping fluence is further increased from 12 μJ/cm^2 to 25 μJ/cm^2 within the ASE regime, the ΔASE is proportionally increased from 22.3 % to 37.8 % (Figure 4b and 4c). The ASE spectra under circular and linear polarization sources at different excitation intensities below and above the threshold are also shown in Figure S2. Thus, the long-range orbit-orbit interaction between coherent light-emitting excitons is largely increased upon increasing pumping density during ASE development in the $CsPbBr_3$ microrods. Figure 5 shows that the orbit-orbit interaction between coherent transition dipoles is realized at a threshold pumping fluence similar to the ASE intensity, shown as a similar trend between ΔASE amplitude and ASE intensity as the pumping intensity is increased. This indicates that the long-range orbit-orbit interaction through orbital polarizations plays an important role in developing coherent interaction between light-emitting excitons towards realizing ASE.

In summary, we have experimentally identified that the orbit-orbit interaction indeed occurs between coherent light-emitting excitons in the ASE regime based on the $CsPbBr_3$ microrods by monitoring ΔASE upon switching the pumping beam between linear and circular polarizations. We observed that circularly and linearly polarized pumping beams with the same fluence generate higher and lower ASE, leading to a positive ΔASE phenomenon in the randomly orientated $CsPbBr_3$ microrods while switching from linear to circular polarization. This positive ΔASE phenomenon provides evidence that the long-range orbit-orbit interaction is realized between coherent light-emitting excitons, increasing ASE in the $CsPbBr_3$ microrods. Essentially, this observation indicates that the relaxation time of long-range orbit-orbit interaction can reach the time window longer than the lifetime of coherent light-emitting excitons in ASE. This provides the time-constant precondition that the long-range orbit-orbit interaction can increase the coherent interaction between light-emitting excitons towards generating an ASE. Furthermore, the similar

trends between ΔASE and ASE amplitudes with increasing pumping intensity indicate that the long-range orbit-orbit interaction plays an important role in developing an ASE in metal halide perovskites.

Methods

Materials: The method to prepare the microrod $CsPbBr_3$ was modified and optimized based on the literature information.[29] The $CsPbBr_3$ precursor solution was prepared by dissolving 0.1 mmol CsBr and $PbBr_2$ (Xi'an p-OLED Inc.) into 1 ml dimethylformamide (Sigma-Aldrich). Then the solution was applied to the ultrasonic treatment for 10 min. For $CsPbBr_3$ microrods growth process, 5 μL solution was dropped on a pre-cleaned glass substrate. Then put the substrate into a sealed glass container with isopropyl alcohol atmosphere for 12 hours, in which the $CsPbBr_3$ microrods start to grow. After the growth process was finished, the substrate was rinsed by the toluene solvent and dried up with nitrogen gas blow.

Characterizations: The optical microscopy images were captured by using the Horiba Xplora Plus system. The excitation and the PL spectra were measured by using the Horiba Fluorolog 3 spectrometer with the Xenon lamp as the excitation source. The ASE spectra were recorded by using the Oceanoptics FLAME-S-XR1-ES spectrograph. The pump beam was from the pulsed laser beam (343 nm) generated through a harmonic generator (Ultrafast Systems LLC, third harmonic) with a Pharos laser (Light Conversion, 1 kHz, 1030 nm, 290 fs). The diameter of the focused laser beam is ~ 60 μm. All the ASE measurements were performed in the transmission geometry with the pump beam and detection direction normal to the sample surface. The time-resolved PL measurements in the ASE regime were token by using the Horiba Fluorolog 3 time-correlated single-photon counting system in combination with the pulsed laser beam (343 nm, 25 kHz, 290 fs). The FWHM of the instrument response function (IRF) is around 180 ps, which can resolve the short lifetime around 18 ps through iterative reconvolution. For the ΔPL measurements in the ASE regime, a linear polarizer combined with the zero-order quarter plate (343 nm) was used to generate a switchable linearly and circularly polarized pump beam with identical intensity.

Acknowledgements

This research was supported by Air Force Office of Scientific Research (AFOSR) under the grant number FA 9550-15-1-0064, AOARD (FA2386-15-1-4104), and National Science Foundation (NSF-1911659). The authors thank the Center for Materials Processing, a Center of Excellence at the University of Tennessee, Knoxville funded by the Tennessee Higher Education Commission (THEC), for financial support (M. W.).

Conflict of Interest

The authors declare no competing financial interests.

Figures

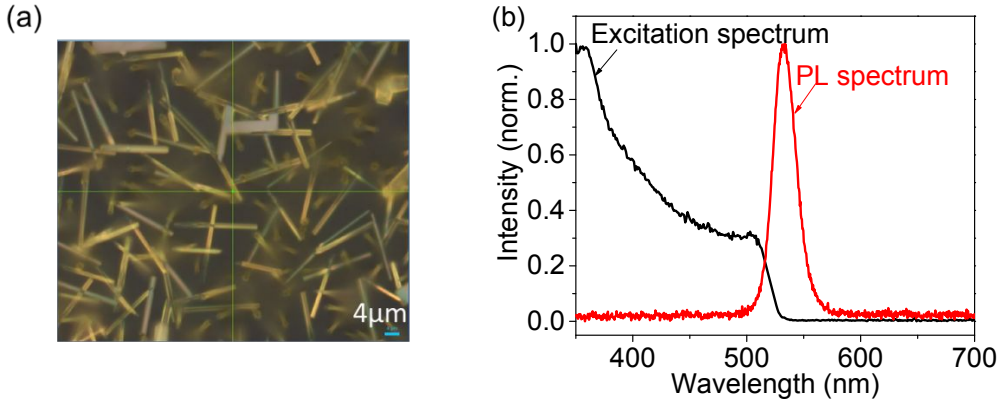

Figure 1. Characterizations on $CsPbBr_3$ microstructures. (a) Optical microscopy image of the $CsPbBr_3$ microrods grown in the glass substrate. (b) excitation and the PL spectra of the $CsPbBr_3$ microrods in glass substrate.

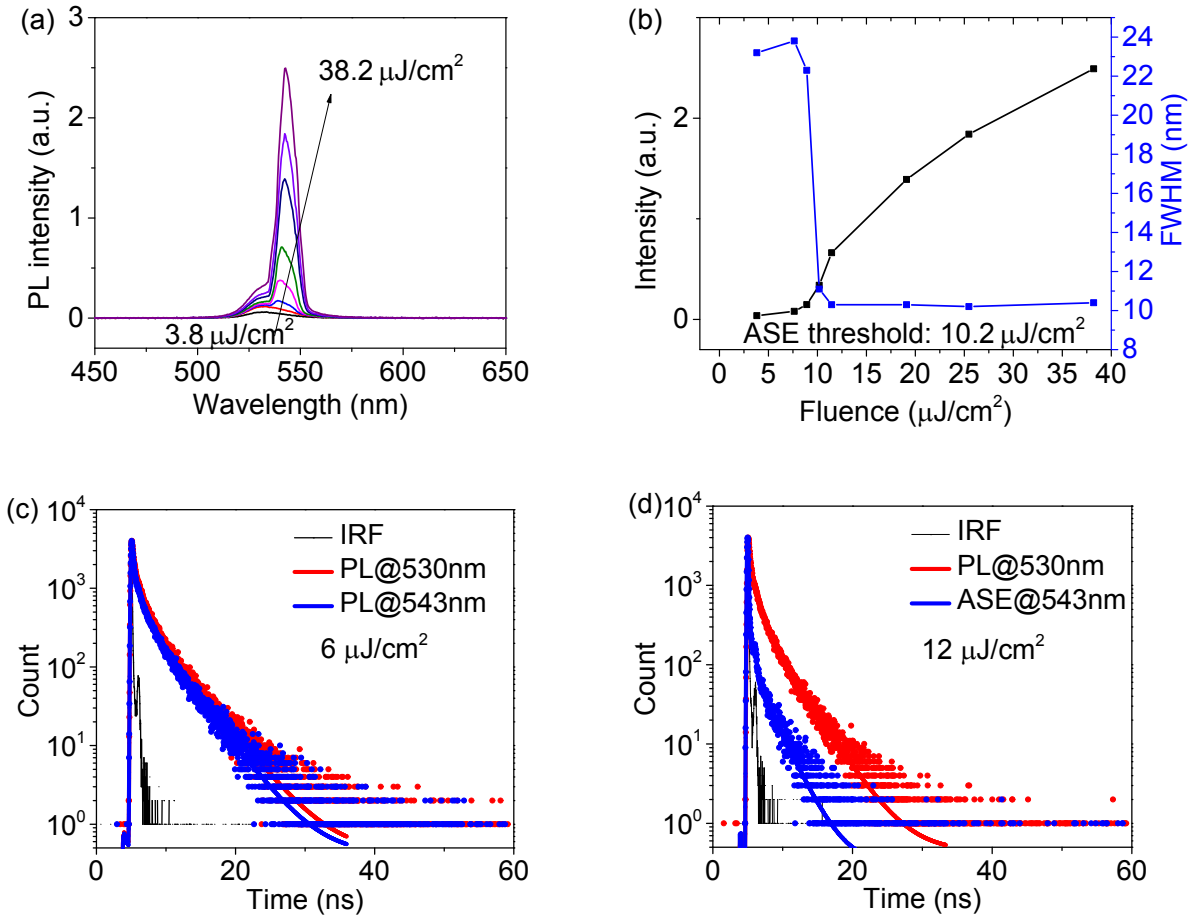

Figure 2. ASE characteristics in cesium perovskite microstructures. (a) PL spectra under different pump fluences measured in transmission mode. (b) Linewidth (FWHM) and ASE intensity against pumping fluence. (c) PL decay curves in ASE region (543 nm) and PL region (530 nm) with the pumping fluence below the ASE threshold. (d) PL decay curves in ASE region (543 nm) and PL region (530 nm) with the pumping fluence above the threshold.

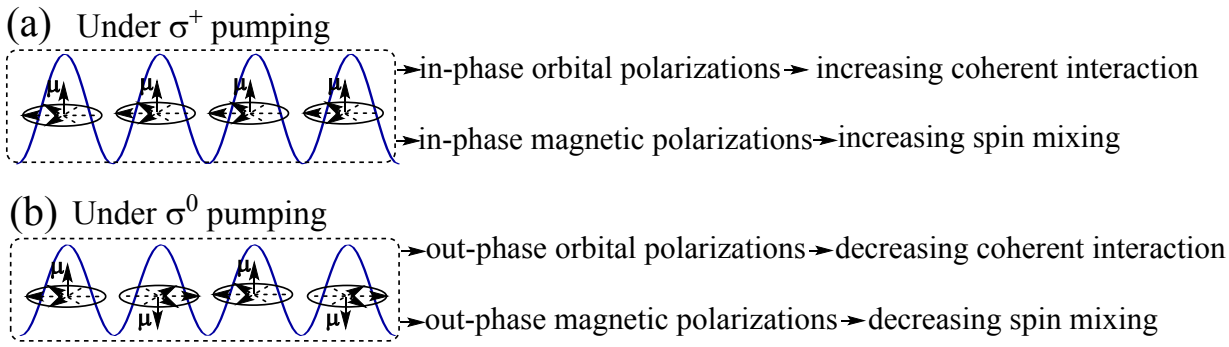

Figure 3. Schematic diagram to show in-phase and out-phase orbit-orbit interactions between light-emitting excitons optically operated by circularly and linearly polarized photoexcitations (σ^+ *and* σ^0). (a) Circularly polarized photoexcitation generates in-phase orbital and magnetic polarizations between light-emitting excitons. In-phase orbital polarizations increase coherent interaction between light-emitting excitons. In-phase magnetic polarizations increase spin-orbital coupling, increasing spin mixing to convert bright excitons to dark excitons. (b) Linearly polarized photoexcitation generates out-phase orbital polarizations between light-emitting excitons. Out-phase orbital polarizations decrease coherent interaction between light-emitting excitons. Out-phase magnetic polarizations decrease spin-orbital coupling, decreasing spin mixing to convert bright excitons to dark excitons.

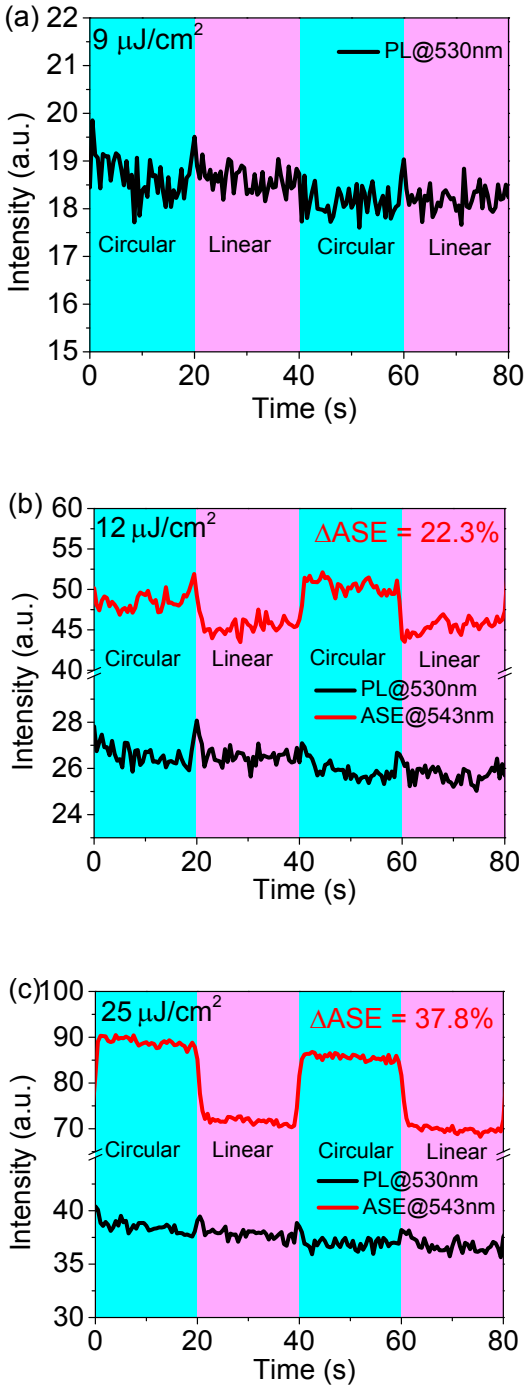

Figure 4. ΔASE and ΔPL simultaneously measured at ASE peak (543 nm) and PL peak (530 nm) with different pumping intensities. (a) Pumping fluence:9 μJ cm^{-2}. (b) Pumping fluence:12 μJ cm^{-2}. (c) Pumping fluence: 25 μJ cm^{-2}.

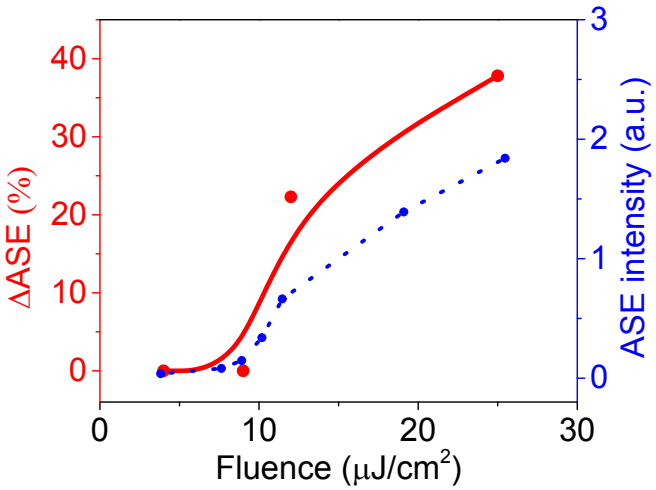

Figure 5. ΔASE signal and ASE intensity as a function of pumping fluence in $CsPbBr_3$ microrods.

References

1. S. Yakunin, L. Protesescu, F. Krieg, M. I. Bodnarchuk, G. Nedelcu, M. Humer, G. De Luca, M. Fiebig, W. Heiss and M. V. Kovalenko, *Nat. Commun.*, 2015, **6**, 8056.
2. G. Xing, N. Mathews, S. S. Lim, N. Yantara, X. Liu, D. Sabba, M. Grätzel, S. Mhaisalkar and T. C. Sum, *Nat. Mater.*, 2014, **13**, 476.
3. H. Zhu, Y. Fu, F. Meng, X. Wu, Z. Gong, Q. Ding, M. V. Gustafsson, M. T. Trinh, S. Jin and X. Zhu, *Nat. Mater.*, 2015, **14**, 636-642.
4. S. Adjokatse, H.-H. Fang and M. A. Loi, *Materials Today*, 2017, **20**, 413-424.
5. K. Roh, L. Zhao, W. B. Gunnarsson, Z. Xiao, Y. Jia, N. C. Giebink and B. P. Rand, *ACS Photonics*, 2019, **6**, 3331-3337.
6. S. A. Veldhuis, P. P. Boix, N. Yantara, M. Li, T. C. Sum, N. Mathews and S. G. Mhaisalkar, *Adv. Mater.*, 2016, **28**, 6804-6834.
7. L. Protesescu, S. Yakunin, M. I. Bodnarchuk, F. Krieg, R. Caputo, C. H. Hendon, R. X. Yang, A. Walsh and M. V. Kovalenko, *Nano letters*, 2015, **15**, 3692-3696.
8. K. Park, J. W. Lee, J. D. Kim, N. S. Han, D. M. Jang, S. Jeong, J. Park and J. K. Song, *J. Phys. Chem. Lett.*, 2016, **7**, 3703-3710.
9. O. Yaffe, A. Chernikov, Z. M. Norman, Y. Zhong, A. Velauthapillai, A. van der Zande, J. S. Owen and T. F. Heinz, *Phys. Rev. B*, 2015, **92**, 045414.
10. P. Brenner, O. Bar-On, M. Jakoby, I. Allegro, B. S. Richards, U. W. Paetzold, I. A. Howard, J. Scheuer and U. Lemmer, *Nat. Commun.*, 2019, **10**, 1-7.
11. Y. Jia, R. A. Kerner, A. J. Grede, B. P. Rand and N. C. Giebink, *Nat. Photonics*, 2017, **11**, 784.
12. C. Qin, A. S. Sandanayaka, C. Zhao, T. Matsushima, D. Zhang, T. Fujihara and C. Adachi, *Nature*, 2020, **585**, 53-57.
13. Z. Yu, *Sci. Rep.*, 2016, **6**, 28576.
14. J. Even, L. Pedesseau, J.-M. Jancu and C. Katan, *J. Phys. Chem. Lett.*, 2013, **4**, 2999-3005.
15. V. V. Belykh, D. R. Yakovlev, M. M. Glazov, P. S. Grigoryev, M. Hussain, J. Rautert, D. N. Dirin, M. V. Kovalenko and M. Bayer, *Nat. Commun.*, 2019, **10**, 1-6.
16. M. Zhou, J. S. Sarmiento, C. Fei, X. Zhang and H. Wang, *J. Phys. Chem. Lett.*, 2020.
17. R. Wang, S. Hu, X. Yang, X. Yan, H. Li and C. Sheng, *J. Mater. Chem. C*, 2018, **6**, 2989-2995.
18. J. Wang, C. Zhang, H. Liu, R. McLaughlin, Y. Zhai, S. R. Vardeny, X. Liu, S. McGill, D. Semenov, H. Guo, R. Tsuchikawa, V. V. Deshpande, D. Sun and Z. V. Vardeny, *Nat. Commun.*, 2019, **10**, 129.
19. Y. Bai, J. Qin, L. Shi, J. Zhang, M. Wang, Y. Zhan, H. Zou, S. Haacke, X. Hou and J. Zi, *Adv. Opt. Mater.*, 2019, 1900345.
20. K.-J. Kim, *Phys. Rev. Lett.*, 1986, **57**, 1871.
21. H. Xu, P. Prabhakaran, S. Choi, M. Wang, K.-S. Lee and B. Hu, *J. Phys. Chem. Lett.*, 2019, **11**, 1-6.
22. M. Wang, H. Zou, J. Zhang, T. Wu, H. Xu, S. Haacke and B. Hu, *J. Phys. Chem. Lett.*, 2020, **11**, 3647-3652.
23. J. Zhang, J. Qin, T. Wu and B. Hu, *J. Phys. Chem. Lett.*, 2020.
24. J. Li, W. Zhou, L. Jiang, Z. Fang, Z. Yang, C. Lin, X. Xu, Z. Ye, H. Zhu and H. He, *J. Mater. Chem. C*, 2019, **7**, 15350-15356.
25. M. L. De Giorgi, A. Perulli, N. Yantara, P. P. Boix and M. Anni, *J. Phys. Chem. C*, 2017, **121**, 14772-14778.
26. J. Pan, S. P. Sarmah, B. Murali, I. Dursun, W. Peng, M. R. Parida, J. Liu, L. Sinatra, N. Alyami and C. Zhao, *J. Phys. Chem. Lett.*, 2015, **6**, 5027-5033.

27. J. Navarro-Arenas, I. Suárez, V. S. Chirvony, A. F. Gualdrón-Reyes, I. Mora-Seró and J. Martínez-Pastor, *J. Phys. Chem. Lett.*, 2019, **10**, 6389-6398.
28. C. Cho, A. Palatnik, M. Sudzius, R. Grodofzig, F. Nehm and K. Leo, *ACS Appl. Mater. Interfaces*, 2020, **12**, 35242-35249.
29. L. Jiang, R. Liu, R. Su, Y. Yu, H. Xu, Y. Wei, Z.-K. Zhou and X. Wang, *Nanoscale*, 2018, **10**, 13565-13571.